Regulation of ramified electrochemical growth by a diffusive wave

Martin Z. Bazant
Department of Physics, Harvard University, Cambridge, Massachusetts 02138
(Received 10 January 1995)

The role of ion transport during ramified growth in a dilute, binary electrolyte is investigated by obtaining a wave solution to effective equations derived by asymptotic analysis of the Nernst transport equations. The concentration profile exhibits a diffusion layer ahead of the growing tips, in agreement with experiment and theory. The non-Laplacian electric field is stronger in the diffusion layer than in the bulk, and cations are accelerated through the layer toward the tips. The well-known growth speed of the aggregate envelope, roughly equal to the speed of migrating anions in the bulk emerges as the characteristic wave speed of our equations. The "copper ratio" is also predicted and is linked to the regulation of growth by the diffusive wave. Finally, an estimate of the induction time for ramified growth is derived, based on the idea that a critical diffusion layer width must be attained.

PACS number(s): 81.15.Pq, 66.10.−x, 68.70.+w, 66.30.Qa

I. INTRODUCTION

The complex morphologies produced by the electrochemical deposition of metal ions from aqueous solution exemplify the subtle and intriguing behavior that a many-body system can exhibit far from equilibrium [1–13]. The case of a dilute, binary electrolyte in the absence of an external mixing agent provides a particularly rich system for experimental and theoretical study. The typical experimental cell consists of a narrow (0.01–0.10 mm) region of electrolyte, (0.01–0.10) M $CuSO_4$ or $ZnSO_4$, confined between two insulating planes. At opposite ends of the cell (in either a radial or parallel geometry), separated by 1–10 cm, are pure metal electrodes of the same type as the cationic species. Deposition is driven either by a constant applied potential of 1–30 V or by a constant current density of 1–50 mA/cm^2. The growth envelope advances with speeds of 0.1–50 μm/sec (corresponding to small and large applied potentials, respectively). Varying the applied potential (or current) and concentration produces a wide range of growth morphologies that have been studied extensively over the last decade.

Theoretical analysis of the growth process typically falls into three categories: stability analysis, Monte-Carlo simulation, and the solution of model partial differential equations. The first involves modeling the stability of a flat interface to shed light on the onset of nonuniform growth [14–16], while the second involves simulations akin to diffusion-limited aggregation to predict growth morphology and microstructure [17–20]. Our investigation follows the third theoretical approach, which involves the solution of various approximate equations of ion transport and deposition kinetics [6,21–27]. An important goal in solving the equations is to link fundamental properties of the electrolyte, such as ion charges and mobilities, to properties of the growth process, such as the speed of the aggregate envelope and perhaps even aspects of the morphology of the deposit. The solution of the transport equations also provides us with a detailed description of ion concentrations and the electrostatic potential (and thus the ion fluxes) that would be difficult to observe experimentally.

Our focus is on the role of transport ahead of the deposit in regulating the advance of established growth, a subject that has been investigated both experimentally and theoretically [1,12,22,23,28–33]. In order to be consistent with previous findings, we would expect an analytic solution to the transport equations to correctly predict the growth speed of the aggregate envelope observed by Fleury *et al.* [33] (and subsequently by others [10,12,22,30]), which is explained by an ohmic transport model. It is found that, especially at high current densities, the growth speed is roughly equal to the migration speed of anions in the bulk electric field. In this paper, we present an asymptotically accurate solution of the Nernst transport equations that does indeed predict the growth speed as well as experimentally observed concentration profiles. Our results include neutrality of the electrolyte (away from the double layers) as well as a non-Laplacian potential.

The assumption of electroneutrality is often invoked to justify Laplace's equation for the electrostatic potential. Indeed, the most common approximations in electrochemistry, the so-called primary and secondary current distributions, involve a Laplacian potential [21,25]. (The former assumes the electrodes to be equipotential surfaces, while the latter includes the Butler-Volmer equation for deposition kinetics.) The use of Laplace's equation is appropriate for a binary electrolyte when either the concentration is uniform (due to convective or mechanical mixing) or the system has reached a steady state, but, as emphasized by Newman [21], electroneutrality does not in general imply a Laplacian potential. Newman's argument has recently been supported by the asymptotic analysis of Bayly *et al.* [34]. The relevant aspects of their work are outlined in Sec. II and provide the starting point for our analysis (in the form of effective

partial differential equations).

Our interest in an accurate description of transport during growth is motivated by experiments in which local concentration measurements are made by optical methods [12,22,24,28,29,32]. Especially in the fractal growth regime, a significant diffusion layer of concentration gradients is observed to precede the growing tips. Moreover, the formation of the diffusion layer is correlated with the onset of nonuniform growth, and once set into motion the concentration profile maintains its shape [29,32]. These observations suggest that ramified growth is a wave phenomenon, whose proper description must include a time-dependent and nonuniform concentration and potential. We emphasize the wave nature of the solution to avoid any confusion caused by the term "moving steady state" used elsewhere in the literature. (The term "dynamic diffusion layer" used by Barkey *et al.* seems more accurate [22,31].) In our analysis, the wave hypothesis is used to extract a solution from the effective partial differential equations presented in the next section, and the characteristic wave speed is identified with the growth speed of the aggregate envelope.

Recent interest in modeling details of transport during ramified growth was sparked by Chazalviel with his steady-state solution to the Nernst transport equations [23]. By keeping the cation and anion concentration as separate variables, the formation of space charges is described. The model equations (without the steady-state approximation used for an analytic solution), however, admit a numerical solution only for unrealistically tiny concentrations (10^{-10} M) [20,23]. The reason for numerical instability at realistic concentrations is that space charges can only exist in thin layers (on the order of micrometers or less) near the electrodes. Thus, by applying the equations to the entire cell the numerical method is forced to resolve dynamics on an overly wide range of length and time scales (fast dynamics in the tiny space charge layers with slow dynamics in the bulk). The same problem was anticipated by Newman in his study of laminar diffusion layers [25]. These results suggest that the more systematic approach of singular perturbation theory is required to describe dynamics in the various regions of the electrolyte, as presented in the next section. The asymptotic analysis captures the essence of the Chazalviel's "regional approximation."

In summary, we present a wave solution to the effective equations of Newman [21] and Bayly *et al.* [34] to describe transport during established ramified growth. For a tractable problem that still contains the essential physics, we specialize to planar electrodes with large enough current to produce fairly dense and homogeneous growth. Under such conditions, a wave solution to the effective equations yields the growth speed, concentration and potential profiles, and ion fluxes. Finally, the induction time for the onset of ramified growth is also estimated using physical arguments.

II. DIMENSIONLESS TRANSPORT EQUATIONS

We begin by outlining the derivation of effective equations for transport in a dilute, binary electrolyte from Nernst transport equations. For details of the analysis and discussion of the results the reader is referred to the paper of Bayly *et al.* [34]. Although their analysis includes matching with the space charge layers, we only address the derivation of the bulk equations, since we will be ignoring the details of transport near the growth. The bulk equations turn out to be the same as those derived by Newman through direct manipulation of the transport equations [21].

The fundamental equations for the cation and anion concentrations, N_+ and N_-, respectively, ignoring gravitational and magnetic effects, are the convection-migration-diffusion equations (ion number conservation),

$$\frac{\partial N_\pm}{\partial t} = -\nabla \cdot (\boldsymbol{u} N_\pm \mp \mu_\pm N_\pm \nabla V - \kappa_\pm \nabla N_\pm), \quad (2.1)$$

where V, $\boldsymbol{u}$, $\mu_\pm$, and $\kappa_\pm$ are the electrostatic potential, fluid velocity, ion mobilities (in units of velocity per electric field), and diffusion coefficients [21,23,34,35]. The potential satisfies Poisson's equation,

$$-\nabla \cdot (\varepsilon \nabla V) = z_+ e N_+ - z_- e N_-, \quad (2.2)$$

where $z_\pm$ are the ion charge numbers and ε is the dielectric coefficient of water. The incompressible Navier-Stokes equations determine the velocity $\boldsymbol{u}$ of the solvent. Because fluid motion is uniform sufficiently far away from the electrodes [26], even during ramified growth, we will ignore the Navier-Stokes equations in the interest of investigating the role of bulk transport during growth. The mobilities and diffusion coefficients are connected by the Einstein relation,

$$\mu_\pm = \frac{z_\pm e}{kT} \kappa_\pm, \quad (2.3)$$

where k is Boltzmann's constant and T the absolute temperature. For dilute solutions, the diffusion coefficients are assumed constant and electric fields outside the double layer are small enough to take the dielectric coefficient to be constant as well [21,36].

The first step in the analysis is to scale all variables by introducing corresponding dimensionless variables (denoted by tilde accents) expected to be of order unity. Concentration is scaled by the number density of salt N_{ref} in the bulk electrolyte before any potential is applied. We assume for convenience of notation that there is only one cation per salt molecule. Distance is scaled to a reference length L_{ref} characteristic of the region of interest. For modeling transport across the cell, a natural choice for L_{ref} is the distance between the electrodes. The reference diffusion coefficient is the average of the cation and anion values weighted by the mobilities of the opposite species [21,24,25,34],

$$\kappa_{ref} = \frac{\mu_+ \kappa_- + \mu_- \kappa_+}{\mu_+ + \mu_-}, \quad (2.4)$$

and potential is scaled by the thermal voltage, $V_{ref} = kT/e$. Finally, the diffusive scales are used for time, velocity, and current,

$$t_{ref} = \frac{L_{ref}^2}{\kappa_{ref}}, \quad u_{ref} = \frac{\kappa_{ref}}{L_{ref}}, \quad J_{ref} = eN_{ref}u_{ref}, \tag{2.5}$$

respectively.

The dimensionless conservation equations do not involve any coefficients. The basis for the asymptotic analysis, however, is the appearance of a huge parameter,

$$A = \left(\frac{L_{ref}}{\lambda_D}\right)^2, \tag{2.6}$$

multiplying the charge in the dimensionless Poisson equation,

$$-\nabla^2\tilde{V} = A\left(z_+\tilde{N}_+ - z_-\tilde{N}_-\right), \tag{2.7}$$

where

$$\lambda_D = \sqrt{\frac{kT\varepsilon}{e^2N_{ref}}} \tag{2.8}$$

is the Debye screening length. For fractal growth, the cell size is on the order of centimeters (and the observed diffusion layer width is several millimeters) [29], while the Debye screening length is on the order of micrometers or less, so that a typical value of A is 10^{10} ($L_{ref} = 1$ cm, $N_{ref} = 0.01$ M, $T = 300$ K). Because the presence of even minuscule space charges spread over macroscopic distances produces enormous electric fields that cannot be supported by the system (expect for very short "relaxation" times), we conclude that macroscopic regions of the electrolyte (with reference length $\gg \lambda_D$) have an overwhelming tendency toward electroneutrality.

Because a tiny parameter A^{-1} multiplies the highest derivative in our equations, the perturbative problem is singular, and asymptotic analysis must involve matching expansions valid in the bulk with separate expansions valid in the boundary layers [37]. By expanding variables in the bulk in powers of A^{-1}, it turns out, not surprisingly, that the zeroth order behavior of the system is electroneutrality, so that we can define a single concentration variable,

$$\tilde{C}(\boldsymbol{x},t) = z_+\tilde{N}_+(\boldsymbol{x},t) = z_-\tilde{N}_-(\boldsymbol{x},t), \tag{2.9}$$

which is the positive (and negative) charge density. The first order behavior of the system involves a convection-diffusion equation for the concentration

$$\frac{\partial\tilde{C}}{\partial t}(\boldsymbol{x},t) + \tilde{\boldsymbol{u}}\cdot\nabla\tilde{C}(\boldsymbol{x},t) = \nabla^2\tilde{C}(\boldsymbol{x},t), \tag{2.10}$$

and an elliptic equation for the potential,

$$\nabla\cdot[\tilde{C}(\boldsymbol{x},t)\nabla\tilde{V}(\boldsymbol{x},t)] = \left(\frac{\kappa_- - \kappa_+}{z_+\kappa_+ + z_-\kappa_-}\right)\nabla^2\tilde{C}(\boldsymbol{x},t), \tag{2.11}$$

which expresses charge conservation. The "ambipolar diffusion equation" for the concentration is derived by Rosso *et al.* by eliminating the potential in the ion conservation equations, Eq. (2.1), using the assumption of quasi-neutrality [24]. Newman derives the potential equation by simply requiring that $\nabla\cdot\tilde{\boldsymbol{J}} = 0$ [21]. Note that the electrostatic potential obeys Laplace's equation, if the concentration is uniform. If we make a quasistatic approximation (or let $\kappa_+ = \kappa_-$), then the equation reduces to $\nabla\cdot(\tilde{C}\nabla\tilde{V}) = 0$, which itself reduces to Laplace's equation if and only if the concentration is uniform.

Analysis is simplified by a change of variables from the electrostatic potential to the anion electrochemical potential,

$$\tilde{\chi}(\boldsymbol{x},t) = \left(\tilde{V}(\boldsymbol{x}) - \tilde{V}_{anode}\right) - \frac{1}{z_-}\ln\tilde{C}(\boldsymbol{x},t). \tag{2.12}$$

In terms of C and χ, the anion flux takes the fairly simple form,

$$\tilde{\boldsymbol{F}}_-(\boldsymbol{x},t) = \tilde{\kappa}_-\tilde{C}(\boldsymbol{x},t)\nabla\tilde{\chi}(\boldsymbol{x},t) + \tilde{\boldsymbol{u}}\frac{\tilde{C}(\boldsymbol{x},t)}{z_-}. \tag{2.13}$$

(Throughout the paper "flux" should be strictly interpreted as "flux density.") The cation flux is

$$\tilde{\boldsymbol{F}}_+(\boldsymbol{x},t) = -\tilde{\kappa}_+\left[\tilde{C}(\boldsymbol{x},t)\nabla\tilde{\chi}(\boldsymbol{x},t) + \left(\frac{z_+ + z_-}{z_+z_-}\right)\nabla\tilde{C}(\boldsymbol{x},t)\right] + \tilde{\boldsymbol{u}}\frac{\tilde{C}(\boldsymbol{x},t)}{z_+}, \tag{2.14}$$

and the form of the potential equation is unaffected by the change of variables,

$$\nabla\cdot\left(\tilde{C}(\boldsymbol{x},t)\nabla\tilde{\chi}(\boldsymbol{x},t)\right) = \alpha\nabla^2\tilde{C}(\boldsymbol{x},t). \tag{2.15}$$

Equations (2.10) and (2.15) are the effective transport equations we must solve. To further simplify the equations, we introduce the dimensionless coefficients

$$\alpha = \frac{\tilde{\kappa}_+\gamma}{\beta}, \quad \beta = z_+\tilde{\kappa}_+ + z_-\tilde{\kappa}_-, \quad \gamma = 1 + \frac{z_+}{z_-}. \tag{2.16}$$

The useful relationship, $z_-\tilde{\kappa}_-\alpha = 1$, can be obtained from the reference scaling for diffusion coefficients, Eq. (2.4). With these definitions the current (taken to be positive when directed in $-\hat{\mathbf{x}}$ direction) is

$$\tilde{\boldsymbol{J}}(\boldsymbol{x},t) = -\beta\tilde{C}(\boldsymbol{x},t)\nabla\tilde{\chi}(\boldsymbol{x},t) - \gamma\tilde{\kappa}_+\nabla\tilde{C}(\boldsymbol{x},t), \tag{2.17}$$

and we note again that the potential equation expresses the requirement that $\nabla\cdot\tilde{\boldsymbol{J}} = 0$.

The argument for electroneutrality breaks down at length scales small enough to make $A \approx 1$. Space charge is confined to microscopic boundary layers (of width $\approx \lambda_D$) separating the bulk electrolyte from electrode surfaces. The space charge region is sometimes called the "diffuse part of the electric double layer" [21], but should not be confused with the macroscopic "diffusion layer" defined below as part of the neutral region. The complexity of growth morphology and the nonlinear effective boundary conditions expressing double layer chemistry motivate us to separate the region of integration from the growth. Thus, in our crude approximation of dynamics near the growth, the asymptotic matching with the space charge layers described by Bayly *et al.* is irrelevant [34].

III. EQUATIONS FOR THE WAVE FORM

For simplicity, we consider only growth processes with planar symmetry across most of the cell ahead of the growing tips so that transport dynamics can be analyzed in one spatial dimension. Our frame of reference for fluid motion and ion flux is the frame of the bulk water solvent, which slowly retreats from the cathode at a constant speed v_{anode} (in the lab frame), the speed of the uniformly dissolving anode surface. Due to the planar symmetry of the system in the bulk it is reasonable to assume that the *cathode hull* (CH), the convex hull of the growth, is a plane parallel to the planes of the initial electrode surfaces. The situation is best realized by dense parallel growth [33], and excludes the extreme case of "dense radial growth [9]". The cathode hull moves at a velocity v with respect to the water ($v + v_{anode} \gg v_{anode} > 0$).

Our picture of the growth process is that a diffusive wave is sweeping through the bulk electrolyte leaving a ramified metal deposit in its wake. In the back region of the wave front (the "active region" discussed below) current, flowing uniformly in the bulk electrolyte, is compressed onto the narrow deposit tips it leaves behind (thus making them grow faster than the anode dissolves). While it may seem impossible at first to have wave propagation in a dissipative system, the diffusion equation does, in fact, allow a wave solution as long as the region of integration is semi-infinite and the boundary surface is advancing at precisely the wave speed [15,22,31,38].

The first step in understanding the growth process is to resolve the concentration and potential profiles of the wave front in the moving frame of the cathode hull. The wave structure is simplest (one dimensional) just ahead of the growing tips where dynamics have approximate planar symmetry and where the water velocity is uniform. Let the *outer cathode hull* (OCH) denote a plane parallel to the cathode hull beyond which complete planar symmetry is assumed. Although current compression occurs in the region behind the OCH, where dynamics are heterogeneous in three dimensions, we will see that transport dynamics in the wave region, beyond the OCH, control the growth speed of the cathode hull (because they control the flux of ions entering the region of current compression).

Let $\xi = x - vt$ label position in the moving frame perpendicular to the initial electrode surfaces, with $\xi = 0$ at the OCH and increasing in the direction of the anode ($\xi > 0$ defines the wave region). In the moving frame the advection-diffusion equation, Eq. (2.10), takes on the familiar form [9,22],

$$-\tilde{v}\frac{d\tilde{C}}{d\xi} = \frac{d^2\tilde{C}}{d\xi^2}, \tag{3.1}$$

while the potential equation, Eq. (2.15), becomes

$$\frac{d}{d\xi}\left(\tilde{C}\frac{d\tilde{\chi}}{d\xi}\right) = \alpha\frac{d^2\tilde{C}}{d\xi^2}. \tag{3.2}$$

Cation and anion fluxes in the frame of the water solvent, $\tilde{F}_+$ and $\tilde{F}_-$, respectively, are found by dropping the advective terms in Eqs. (2.13) and (2.14). Fluxes in the wave frame involve fictitious advective fluxes due to frame motion

$$\tilde{F}_-^w(\xi) = \tilde{\kappa}_-\tilde{C}(\xi)\frac{d\tilde{\chi}}{d\xi}(\xi) - \tilde{v}\frac{\tilde{C}(\xi)}{z_-}, \tag{3.3}$$

$$\tilde{F}_+^w(\xi) = -\tilde{\kappa}_+\left[\tilde{C}(\xi)\frac{d\tilde{\chi}}{d\xi}(\xi) + \frac{\gamma}{z_+}\frac{d\tilde{C}}{d\xi}(\xi)\right] - \tilde{v}\frac{\tilde{C}(\xi)}{z_+}. \tag{3.4}$$

(In our notation, fluxes without superscripts are in the frame of the solvent, while superscript w denotes fluxes in the wave frame.) Because the electrolyte is neutral, the current is the same in the solvent and wave frames. From the expressions for the fluxes in the wave frame, we can show explicitly that Eq. (3.2) requires that the current is constant, thus preserving electroneutrality during time evolution.

IV. BOUNDARY CONDITIONS

It is observed that the concentration remains uniform across most of the cell during the course of a ramified growth experiment [28,29]. Indeed, deposits typically advance on the scale of minutes or less, while the diffusion time across the cell is on the order of hours. Since the concentration evolves according to a pure diffusion equation, we expect that the concentration will always be equal to the initial bulk value across most of the cell with gradients confined to a narrow diffusion layer near the OCH. (As stated earlier, the diffusion layer is still much wider than the space charge layer.) In terms of the scaled variables, we are led to the boundary condition

$$\lim_{\xi\to\infty}\tilde{C}(\xi) = z_+. \tag{4.1}$$

The semi-infinite region of integration, along with the moving boundary, is mathematically essential for the realization of a diffusive wave.

Because the concentration is uniform in the bulk, Laplace's equation determines the bulk potential. Assuming planar symmetry, this implies that the potential is linear and the electric field constant (directed toward the cathode). The lack of diffusion in the bulk implies that the bulk current must be driven exclusively by a uniform electric field,

$$\tilde{E}_{bulk} \equiv \lim_{\xi\to\infty}\frac{d\tilde{V}}{d\xi} = \lim_{\xi\to\infty}\frac{d\tilde{\chi}}{d\xi} = \frac{\tilde{J}}{z_+\beta}, \tag{4.2}$$

yielding the boundary condition

$$\lim_{\xi\to\infty}\beta\tilde{C}(\xi)\frac{d\tilde{\chi}}{d\xi}(\xi) = \tilde{J}, \tag{4.3}$$

where $\tilde{J}$ is the applied current for galvanostatic experiments ($\tilde{J} > O$ for current toward the cathode in the $-x$ direction). For potentiostatic experiments, $\tilde{J}$ is a free parameter in these equations that can be determined by transport dynamics and chemical reactions at the anode.

Because we know that the anions do not deposit, we should be able to determine the flux of anions in the wave

frame at the OCH, $\tilde{F}_a^w$, so that we have the boundary condition

$$-\tilde{\kappa}_-\tilde{C}(0)\frac{d\tilde{\chi}}{d\xi}(0)+\tilde{v}\frac{\tilde{C}(0)}{z_-}=\tilde{F}_a^w. \tag{4.4}$$

($\tilde{F}_a^w > 0$ for flux toward cathode.) In ramified growth, the only surfaces of active deposition are at the tips most exposed to the bulk electrolyte. The remaining surfaces behind the cathode hull are inactive due to screening of the electric field and concentration gradients by the tips and to fluid motion, which carries ions to the tips [26].

To separate the inactive region from the active region of current compression and deposition, we define the *inner cathode hull* (ICH), a plane behind the growth tips that is parallel to the CH. Like the OCH, the exact placement of the ICH is not well defined since both are simply theoretical constructs. See Fig. 1 for a diagram of the various regions of the electrolyte in our model.

Assuming that the anion population of the active region (between the ICH and the OCH) remains constant in time, the squeezing of anion flux from the bulk into the narrower region between the tips must cause an increase in anion flux in the wave frame,

$$(1-\tau)\,\tilde{F}^w_{-ICH}=-\tilde{F}_a^w, \tag{4.5}$$

where we have thus defined the *tip fraction* $0 < \tau < 1$, an effective area of the ICH plane occupied by the cross section of the ramified growth. By construction, the anion (and cation) flux is zero in the lab frame at the ICH, so,

$$\tilde{F}^w_{-ICH}=-\left(\tilde{v}+\tilde{v}_{anode}\right)\tilde{N}_{ICH}\approx-\frac{z_+}{z_-}\tilde{v}\tilde{N}_{ICH}, \tag{4.6}$$

where we have assumed one cation per salt molecule and approximated $v \gg v_{anode}$. Now we have the flux,

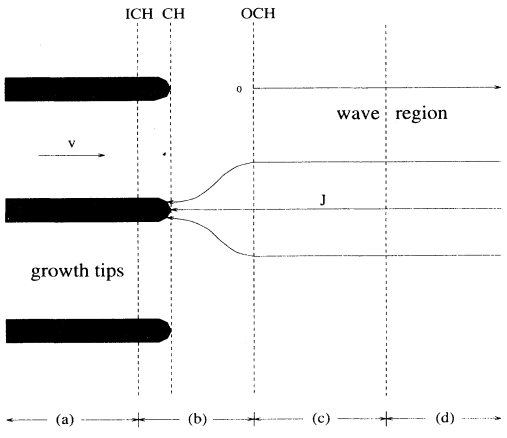

FIG. 1. The regions of the electrolyte in our model of ramified growth: (a) the inactive region, (b) the active region, (c) the diffusion layer, and (d) the bulk. The region of integration ($\xi > 0$) is labeled as the wave region. The cathode hull (CH) and inner (ICH) and outer (OCH) cathode hulls are also shown. Lines of current are shown indicating compression in the active region.

$$\tilde{F}_a^w=\frac{z_+}{z_-}\tilde{v}\tilde{N}_{ICH}\left(1-\tau\right), \tag{4.7}$$

that we need to specify the first boundary condition at the OCH.

To complete the bookkeeping of ions crossing the active region, we have the conservation of cations,

$$-\left(1-\tau\right)\tilde{v}N_{ICH}-\tau R_{dep}=\tilde{F}^w_{+OCH}, \tag{4.8}$$

where R_{dep} is the flux of depositing cations at the surface of the active growth tips. While, of course, the deposition flux may vary along the surface, we assume it to be uniformly distributed across the effective tip area given by τ. Equation (4.8) is used to determine τ in Sec. VII.

We now have two second order equations with three boundary conditions. At least one more condition is needed at the OCH. Its derivation must in some way incorporate the current compression and deposition reaction kinetics in the active region and will be addressed in Sec. VII. The net effect of the fourth boundary condition, however, is only to determine the additive constant in the potential, so we can proceed without it for now.

V. THE ROLE OF ANIONS

A wave solution to our equations, Eqs. (3.1) and (3.2), has the property that the anion flux in the moving frame must be uniform across the wave region

$$\tilde{\kappa}_-\tilde{C}(\xi)\frac{d\tilde{\chi}}{d\xi}(\xi)-\tilde{v}\frac{\tilde{C}(\xi)}{z_-}=-\tilde{F}_a^w, \tag{5.1}$$

independent of the boundary conditions used. The wave speed is determined by substituting the bulk electric field into Eq. (5.1),

$$\tilde{v}=z_-\tilde{\kappa}_-\tilde{E}_{bulk}+\frac{z_-}{z_+}\tilde{F}_a^w. \tag{5.2}$$

The first term is the migration speed of anions in the bulk, and the second is a correction when the growth tips are spaced widely enough to allow significant penetration of ions into the inactive region.

The wave speed is a fundamental property of the transport equations and does not depend on our approximation of the active region. As such, it may seem that our result violates the symmetry between anions and cations in transport. Indeed, it is only boundary conditions expressing double layer kinetics that favor cation deposition and introduce asymmetry between the ionic species. As far as the transport equations are concerned, there is no reason to exclude the possibility of anions depositing and cations remaining inactive. In fact, such a solution exists as well. In the next section it is shown that the cation flux $\tilde{F}_+^w$ is also constant in the wave frame. By an analogous argument, the wave speed would be equal to the cation bulk migration speed if $\tilde{F}_+^w = 0$ [see Eq. (6.8)].

If we use our crude expression Eq. (4.7) for the anion flux, then the result for the wave speed is

$$\tilde{v}=\frac{z_-\tilde{\kappa}_-\tilde{E}_{bulk}}{1-\tilde{N}_{ICH}\left(1-\tau\right)}. \tag{5.3}$$

In cases where the ion concentration in the inactive region between tips is negligible, the wave speed is simply the migration speed of anions in the bulk electric field. Fleury *et al.* [1,33] arrive at the same result for galvanostatic cells by experimental observation and physical intuition: in order to avoid the accumulation of space charge, it is necessary for the wave front to advance at precisely the speed with which anions are removed from the region of the growth by the bulk electric field. A more mathematical derivation is presented by Barkey *et al.* to model potentiostatic cells with circular geometry [22], and they also predict the effect of nonzero concentration between the tips. The model of Fleury *et al.* has also been generalized by Trigueros *et al.* to account for the presence of additional inert ionic species [12].

VI. RESOLUTION OF THE WAVE FORM

The diffusion equation, Eq. (3.1), can be easily integrated using the boundary condition, Eq. (4.1), to get the concentration field,

$$\tilde{C}(\xi) = z_+ \left(1 - \tilde{K} e^{-\tilde{v}\xi}\right), \tag{6.1}$$

where $\tilde{K}$ is a constant of integration. The concentration is uniform in the bulk with gradients confined to a diffusion layer near the growth whose width λ (sometimes called the "Nernst layer width" [15] or "diffusion length" [9]) is inversely proportional to the wave speed and proportional to the effective diffusion coefficient (from the scaling). Although the diffusive-wave concentration profile ahead of established growth is well known [22,31,32], there does not seem to be a consensus in the literature on the potential profile.

The potential equation, Eq. (3.2), can be integrated to show that the current is also uniform across the wave region,

$$\beta \tilde{C}(\xi) \frac{d\tilde{\chi}}{d\xi}(\xi) + \gamma \tilde{\kappa}_+ \frac{d\tilde{C}}{d\xi}(\xi) = \tilde{J}. \tag{6.2}$$

(Note that since the current and anion flux are uniform in the moving frame, the cation flux in the moving frame must also be uniform.) When the solution for the concentration is substituted into Eqs. (5.1) and (6.2), which impose the boundary conditions on the anion flux at $\xi = 0$ and on the current at $\xi \to \infty$, respectively, the following relationship is obtained:

$$\alpha z_+ \tilde{v} = \frac{\tilde{J}}{\beta} + \frac{\tilde{F}_a^w}{\tilde{\kappa}_-}, \tag{6.3}$$

which shows that Eq. (5.1) and Eq. (6.2) are not independent. Therefore, one condition is extraneous since it does not determine a constant of integration, and a new condition is needed. This should not be surprising, however, since one condition was needed to find the wave speed.

The required new condition can be produced by simply specifying the salt concentration $\tilde{N}_{OCH}$ at the OCH, because $\tilde{K} = 1 - \tilde{N}_{OCH}$. While it might seem that $\tilde{N}_{OCH}$ should be determined by the equations and not left as a free parameter, we must recognize that one artificial degree of freedom is added to the system by the placement of the OCH. By keeping the active region outside the region of integration, we lose information that we cannot hope to regain without working harder.

The chemical potential is obtained by integrating Eq. (6.2) from 0 to ξ and using Eq. (6.3) to simplify the result,

$$\tilde{\chi}(\xi) = \tilde{E}_{bulk}\xi - \alpha\tilde{v}\,(1-\tau)\,\tilde{N}_{ICH} \ln\left(\frac{1 - \tilde{K}e^{-\tilde{v}\xi}}{1-\tilde{K}}\right) \tag{6.4}$$

and the electrostatic potential is obtained by adding $\tilde{V}_{anode} + \frac{1}{z_-}\ln\tilde{C}(\xi)$. Since $\tilde{N}_{ICH} \ll 1$ for most growth morphologies, the chemical potential is nearly linear across the entire wave region, while the electrostatic potential has an additional steep logarithmic dependence in the diffusion layer. Observe that there turns out to be no new integration constant; the only undetermined parameter is $\tilde{N}_{OCH} = 1 - \tilde{K}$, the same constant from integration of the concentration. This implies a relationship between the concentration and potential at the OCH that precludes the necessity of an additional boundary condition.

The ion fluxes in the solvent frame,

$$\tilde{F}_-(\xi) = \frac{z_+}{z_-}\tilde{v}\left(1 - \tilde{K}e^{-\tilde{v}\xi} - (1-\tau)\,\tilde{N}_{ICH}\right), \tag{6.5}$$

$$\tilde{F}_+(\xi) = -z_+\tilde{\kappa}_+\tilde{E}_{bulk} - \tilde{K}\tilde{v}e^{-\tilde{v}\xi}, \tag{6.6}$$

are obtained by adding fictitious fluxes due to frame motion to the constant fluxes in the wave frame,

$$\tilde{F}_-^w(\xi) = -\frac{z_+}{z_-}(1-\tau)\,\tilde{N}_{ICH}\tilde{v}, \tag{6.7}$$

$$\tilde{F}_+^w(\xi) = -(\tilde{v} + z_+\tilde{\kappa}_+\tilde{E}_{bulk})\tilde{N}_{ref}. \tag{6.8}$$

(Note that $\tilde{N}_{ref} = 1$ is omitted elsewhere in the paper.) Using the cation flux, we can calculate the fraction of the current carried by the cations in the solvent frame,

$$\frac{-z_+\tilde{F}_+(\xi)}{\tilde{J}} = \left(1 + \frac{\mu_-}{\mu_+}\right)^{-1} + \left(1 + \frac{\mu_+}{\mu_-}\right)^{-1}\left(1 - \tilde{N}_{ICH}\right)\tilde{K}e^{-\tilde{v}\xi}. \tag{6.9}$$

In the case $\tilde{N}_{OCH} = \tilde{N}_{ICH} = 0$, this reduces to

$$\frac{-z_+\tilde{F}_+^w(\xi)}{\tilde{J}} = t_+ + t_-e^{-\tilde{v}\xi}, \tag{6.10}$$

where t_+ and t_- are the cation and anion transference numbers, respectively [21],

$$t_\pm = \frac{\mu_\pm}{\mu_+ + \mu_-}. \tag{6.11}$$

Since the transference numbers are the fractions of the

bulk migratory current carried by the two ion species, we see that as the diffusion layer is entered from the bulk, the cations slowly take over the anionic contribution to the current until the current is exclusively cationic at the OCH.

A detailed picture of ion dynamics in the wave region emerges from the consideration of ion velocities in the solvent frame,

$$\tilde{v}_- = \tilde{v}\left(1 - \frac{(1-\tau)\,\tilde{N}_{ICH}}{1 - \tilde{K}e^{-\tilde{v}\xi}}\right) \tag{6.12}$$

$$= \frac{z_-\tilde{\kappa}_-\tilde{E}_{bulk}}{1 - \tilde{K}e^{-\tilde{v}\xi}}\left(1 - \frac{\tilde{K}e^{-\tilde{v}\xi}}{1 - (1-\tau)\,\tilde{N}_{ICH}}\right), \tag{6.13}$$

$$\tilde{v}_+ = -\frac{z_+\tilde{\kappa}_+\tilde{E}_{bulk} + \tilde{K}\tilde{v}e^{-\tilde{v}\xi}}{1 - \tilde{K}e^{-\tilde{v}\xi}}. \tag{6.14}$$

If $\tilde{N}_{ICH} = 0$, then throughout the wave region the anions move at a constant velocity toward the anode equal to the migration velocity in the bulk electric field (which is also the wave velocity). If $\tilde{N}_{ICH} > 0$, then while the bulk speed is unchanged, it is now smaller than the wave speed. Near the growth tips, the anions move even slower than the bulk speed, but still toward the anode (since we expect $\tilde{N}_{ICH} \leq 1$). The interpretation is that when $\tilde{N}_{ICH} > 0$ the tips are overtaking some anions that ultimately end up sitting motionless in the inactive region behind the tips. Cations in the bulk move toward the cathode at the migration velocity in the bulk electric field. Closer to the tips, however, cations are sucked in toward the growth at a greater speed due to the increase in electric field.

VII. CURRENT COMPRESSION AND THE METAL RATIO

Ramified growth occurs because the spatially uniform current in the wave region beyond the OCH is compressed in the active region leading to a flux density of depositing cations at the growth tips that is much greater than the flux density of dissolving metal atoms at the anode. There are a wide variety of mechanisms that can play a role in current compression. In the regime of steady electromigration or diffusion, exposed structures screen the Laplacian field and thus attract incoming cations [3,9,16,18–20,38]. Spatial variations in overpotential and deposition reaction rates on the growth surface [18] and the surface diffusion of adsorbed metal atoms [14] can also influence current compression. A minor role may also be played by surface tension and lattice anisotropy in the regime of validity of our model [11]. There is growing theoretical and experimental evidence, however, that fluid motion is the primary mechanism for current compression in established growth, especially at large applied currents [1,26,39]. Cations are swept toward the tips along "funnels" created by pairs of counter-rotating vortices in the solvent that are driven by electroconvection.

While the details of current compression are of primary concern for understanding the growth morphology, our goal is to understand how transport ahead of the tips influences growth by regulating the arrival of cations. As far as bulk transport is concerned, the net effect of the active region is simply to compress current entering from the bulk by a factor,

$$f \equiv \frac{J_{CH}}{J_{bulk}} = \frac{v_{CH}}{v_{anode}}. \tag{7.1}$$

(the speeds are in the lab frame). We have used the fact that because the anode dissolves uniformly, the current density in the bulk is the same as at the anode surface. The wave speed is related to f by,

$$\tilde{v} = \tilde{v}_{CH} - \tilde{v}_{anode} = (f-1)\tilde{v}_{anode}. \tag{7.2}$$

The speed of the retreating anode surface, assuming uniform dissolution, is

$$\tilde{v}_{anode} = \frac{\tilde{J}}{z_+\tilde{N}_{metal}}, \tag{7.3}$$

where N_{metal} is the number density of metal ions in the electrodes. Equating the current leaving the anode with that entering the cathode and observing that the area of the growing tips is much smaller than the area of the anode for established growth, we conclude that $f \gg 1$. Combining the preceding equations with Eqs. (4.2) and (5.3), we obtain an equation for f,

$$f = \frac{\tilde{N}_{metal}}{\left(1 + \frac{\mu_+}{\mu_-}\right)\left(1 - (1-\tau)\,\tilde{N}_{ICH}\right)}. \tag{7.4}$$

Note that f and τ are related, since current compression must surely be related to the surface area of the active tips. If $\tau = 1$, then growth is uniform, and hence we expect no current compression, $f = 1$. If $\tau \ll 1$, then current must be greatly compressed in the active region, $f \gg 1$.

To arrive at the relationship between f and τ, observe that knowing f gives us the current at the tips (just outside the space charge layer) which can be equated to the deposition flux rate,

$$\tilde{J}_{CH} = f\tilde{J} = z_+\tilde{R}_{dep}. \tag{7.5}$$

Substituting for $\tilde{R}_{dep}$ in Eq. (4.8) and using the (constant) cation flux in the wave frame, Eq. (6.8), yields,

$$\tau f = 1. \tag{7.6}$$

We could have derived this result heuristically as follows. Since no current passes between the active growth tips, the uniformly distributed current at the OCH is compressed into an area that is smaller by a fraction τ after passing through the active region. Current conservation across the active region then implies that $f = \tau^{-1}$.

Now we can eliminate τ in the expression for the current compression factor,

$$f = \left(\frac{\tilde{N}_{metal}}{1 + \frac{\mu_+}{\mu_-}} - \tilde{N}_{ICH}\right)\left(1 - \tilde{N}_{ICH}\right)^{-1}. \tag{7.7}$$

Similarly, we can use our knowledge of f, to eliminate the parameter τ from all our previous results. The only remaining unknown in the expression for f is the parameter N_{ICH}. The concentration in the inactive region between the tips is an acceptable control parameter in any theory that does not track growth from its onset, and is used by Barkey *et al.* [22].

The information about ion conservation captured by the current compression factor can be expressed in another way. Fleury and co-workers define the "copper ratio," which we will call the "metal ratio" M for generality, to be the ratio of the mass of the deposit to the mass of cations at the bulk concentration that would occupy the same volume as the deposit (between the initial cathode surface and the cathode hull) [1,33]. By charge conservation, the mass of the deposit must equal the total mass of the anode metal that has dissolved, so,

$$M = \frac{v_{anode} N_{metal}}{v_{CH} N_{ref}} = \tau \tilde{N}_{metal}. \tag{7.8}$$

Specializing to dense growth ($N_{ICH} = 0$), we recover Fleury's result,

$$M = 1 + \frac{\mu_+}{\mu_-}. \tag{7.9}$$

See Ref. [1] for an interpretation of M.

VIII. SUMMARY OF RESULTS WITH DIMENSIONS

The growth speed is

$$v = \frac{fJ}{z_+ e N_{metal}} = \mu_- E_{bulk} \left(1 - (1-\tau)\frac{N_{ICH}}{N_{ref}}\right)^{-1}, \tag{8.1}$$

where

$$f = \left(\frac{N_{metal}}{1 + \frac{\mu_+}{\mu_-}} - N_{ICH}\right)(N_{ref} - N_{ICH})^{-1} \tag{8.2}$$

is the current compression factor and $\tau = f^{-1}$ the tip fraction. The metal ratio is $M = N_{metal}/(f N_{ref})$. The bulk electric field is related to the current by

$$E_{bulk} = \frac{J}{z_+ e\,(\mu_+ + \mu_-)\,N_{ref}}. \tag{8.3}$$

(Recall the convention that there is one cation per salt molecule, which, if relaxed, would simply mean that we take the number density of cations in the bulk to be our reference concentration N_{ref} rather than the salt concentration.) The cation concentration (number density) exhibits a diffusion layer ahead of the tips,

$$N_+(\xi) = N_{ref} - (N_{ref} - N_{OCH})\, e^{-\frac{v\xi}{\kappa_{ref}}}. \tag{8.4}$$

Due to quasineutrality, the anion concentration is simply, $N_-(\xi) = \frac{z_+}{z_-} N_+(\xi)$. The electrostatic potential provides a constant electric field in the bulk with an increase in the diffusion layer,

$$V(\xi) = V_{anode} + E_{bulk}\xi + \frac{\kappa_-}{\mu_-} \ln\left(\frac{z_+ N_+(\xi)}{N_{ref}}\right) + V_0(\xi), \tag{8.5}$$

where $V_0(\xi)$ is the change in potential due to a nonzero concentration in the inactive region,

$$V_0(\xi) = \left(1 + \frac{z_+}{z_-}\right)\left(1 + \frac{\mu_+}{\mu_-}\right)(1-\tau)\left(\frac{\kappa_+ L_{ref}}{\mu_+ \kappa_{ref} N_{ref}}\right) \times v N_{ICH} \ln\left(\frac{N_+(\xi)}{N_{OCH}}\right). \tag{8.6}$$

[Recall that $N_{OCH} = N_+(0)$.] The cation and anion fluxes in the frame of the solvent are,

$$F_+(\xi) = -\mu_+ N_{ref} E_{bulk} - v\,(N_{ref} - N_{OCH})\, e^{-\frac{v\xi}{\kappa_{ref}}}, \tag{8.7}$$

$$F_-(\xi) = v N_-(\xi) - (1-\tau)\frac{z_+}{z_-} N_{ICH}. \tag{8.8}$$

For many cases of ramified growth, especially dense growth at large currents, the preceding formulas can be simplified by setting $N_{ICH} = 0$. The inclusion of N_{ICH} allows us to see how the diffusion layer adjusts to cases of sparse growth at low currents. The results are valid for both galvanostatic and potentiostatic cells.

By considering various limits of the solution, we can better understand approximations made in other models. The relevant dimensionless parameter is the ratio of the reference and diffusion lengths,

$$b = \frac{v L_{ref}}{\kappa_{ref}}. \tag{8.9}$$

A similar parameter called the Péclet number is used in the study of laminar diffusion layers [25]. However, in that case, the velocity is due to forced convection of the solvent, not diffusive wave propagation. In the limit of small growth speed ($b \ll 1$), the concentration is roughly linear, $N_+ \approx N_{OCH} + (N_{ref} - N_{OCH}) v\xi/\kappa_{ref}$, (satisfying Laplace's equation), while the potential is dominated by the first logarithmic term. (In that limit, however, one must consider the effect of the diffusion layer interacting with the accumulation layer at the anode, the Hecker effect [1,4,9,40].) In the opposite limit of large growth speeds ($b \gg 1$), the diffusion layer is very small, and beyond it the concentration is uniform, $N_+ \approx N_{ref}$, with a linear potential (satisfying Laplace's equation). There may also be situations where the concentration drop across the diffusion layer is negligible and dynamics are controlled by processes in the active region (as in the

analysis of Fleury *et al.* In that case, $N_{OCH} \approx N_{ref}$, and once again the concentration is uniform, and the potential satisfies Laplace's equation in our region of integration.

The relationship between the current and the potential difference across the cell is contained in the relationship between J and N_{OCH} (in turn related to V_{OCH}), which can only be determined by matching our solution to solutions for the active region and the accumulation region near the anode. The constant N_{OCH} must be determined by matching the diffusion layer solution with a solution for the active region, and is influenced by the exact placement of the OCH. Such matching would relate N_{OCH} to $V_{cathode}$ (which is contained in an effective boundary condition expressing deposition reaction kinetics [34]).

IX. THE ONSET OF RAMIFIED GROWTH

We have argued that ramified growth is regulated by a diffusive wave in the electrolyte ahead of the tips. The wave solution exists if and only if the diffusion layer has the critical width,

$$\lambda_c(J) = \frac{\kappa_{ref}}{v} = \frac{\kappa_{ref}}{\mu_- E_{bulk}}, \tag{9.1}$$

where the wave speed v is determined by the current. Note that we have set $N_{ICH} = 0$ because at the onset of growth the inactive region does not yet exist. In galvanostatic cells, the critical width is predetermined by fundamental parameters of the system. The situation is more complicated, however, in potentiostatic cells because current (and hence E_{bulk}) variation causes the critical width to be time dependent.

When the potential or current is applied, thus initiating deposition, the concentration, originally uniform, forms a diffusion layer of increasing width $\lambda(t)$ against the cathode surface due to the deposition of cations and the migratory expulsion of anions [24]. According to our theory, sustained ramified growth is forbidden as long as $\lambda(t) < \lambda_c$, and, therefore, deposition is uniform at first. Once the diffusion layer attains the critical width $\lambda \approx \lambda_c$, transport dynamics permit the sustained magnification of surface instabilities and the ramified growth wave is created and set into motion. Concentration evolution during in a typical experiment in the fractal growth regime is depicted qualitatively in Fig. 2.

Because anions depart the vicinity of the cathode at a rate determined exclusively by the current, we have arrived at an intriguing result: the onset of ramified growth, while driven by a wide variety of mechanisms described in Sec. VII and in the surface instability literature, is regulated by the steady migration of anions in the bulk. By solving the effective equations, Eqs. (2.10) and (2.15), (with boundary conditions from Ref. [34]) in one dimension from the moment when the current is applied and the concentration is uniform, we could determine the time it takes for the diffusion layer to attain the critical width, which, according to our theory, is approximately the induction time t_c. The equations have been solved for $t < t_0$ (when the concentration drops to zero at the cathode) in the case of a galvanostatic cell [24,41]. There is evidence that gravity-induced fluid motion (and possibly also electroconvection) plays an important role in the early stages of the experiments [24,32], so an accurate description must involve the full set of effective equations, including fluid motion [34].

Although obtaining a complete description of the initial concentration evolution is a formidable analytical or numerical task, we can get a reasonable estimate of t_c by using a few simplifying assumptions suggested by theory and experiment. The time scale in the space charge layer is so small that the layer is always in quasi-equilibrium with the neutral electrolyte [34]. Moreover, although there is a significant potential difference across the space

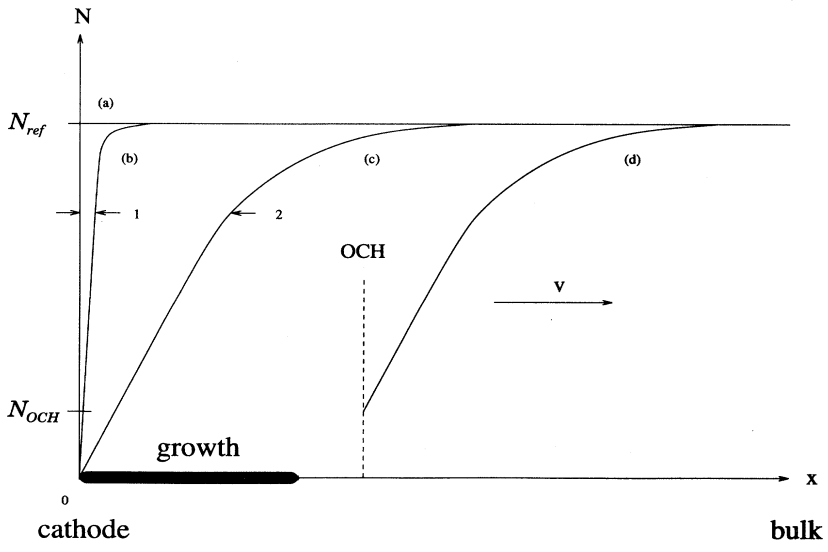

FIG. 2. The evolution of the cation (and anion) concentration from the beginning of the experiment: (a) at $t = 0$ the concentration is uniform, (b) after a small time $t = t_0$ a narrow depletion layer of width λ_0 (1) is formed, (c) at $t = t_c$ the diffusion layer reaches the critical width λ_c (2), and instabilities can be sustained and magnified, and (d) the diffusive wave propagates with the critical layer width.

charge layer at the cathode [23,33], the number of ions responsible for the space charge is much smaller than the number involved in creating the diffusion layer (because $\lambda_D \ll \lambda_c$). Therefore, we are led to neglect the accumulation of charge in the space charge layer so that the change in anion concentration in the diffusion layer is determined by bulk migration alone,

$$\frac{d}{dt}\int_0^\infty N_-(x,t)dx = -\frac{z_+}{z_-}N_{ref}\mu_- E_{bulk}. \qquad (9.2)$$

The function $N_-(x,t)$ should come from a solution to the effective equations, but for simplicity we will use the experimentally determined concentration profile preceding the onset of fractal growth measured by Cork, Pritchard, and Tam [29].

After the experiment begins, the concentration in the immediate vicinity of the cathode falls from the bulk value (≈ 0.5 M) to nearly zero in a brief time t_0 (<1 sec), forming a diffusion layer of width λ_0 (≈ 0.1 mm), roughly independent of applied potential (1–10 V) and gap spacing (25–102 μm). For $t > t_0$, however, the concentration profile seems well approximated by the self-similar form,

$$N_-(x,t) = \frac{z_+}{z_-}N_{ref}\left(1 - e^{-\frac{x}{\lambda(t)}}\right). \qquad (9.3)$$

Substitution of Eq. (9.3) into Eq. (9.2) yields,

$$\lambda(t) = \lambda_0 + \mu_- \int_{t_0}^{t} E_{bulk}(\tau)d\tau. \qquad (9.4)$$

For galvanostatic cells, E_{bulk} is constant [see Eq. (8.3)], so for $t > t_0$ the depletion layer width grows linearly at the speed of the anions (as it must to avoid charge accumulation). However, the potentiostatic data we are using also indicates linear growth of the depletion layer [29], so we will proceed with the assumption that E_{bulk} is constant. Equating with the critical length λ_c, we obtain an estimate for the induction time,

$$t_c = t_i + t_0 - \frac{\lambda_0}{\mu_- E_{bulk}} + \frac{\kappa_{ref}}{(\mu_- E_{bulk})^2}, \qquad (9.5)$$

where t_i accounts for any extra time needed for the magnification of surface instabilities once the critical diffusion layer width has been attained. Since E_{bulk} is not measured experimentally, we express the time to form the critical diffusion layer width in terms of the current,

$$t_c - t_i = t_0 + \left(1 + \frac{\mu_+}{\mu_-}\right)\left[\kappa_+\left(1 + \frac{z_+}{z_-}\right)\left(\frac{z_+ e N_{ref}}{J}\right)^2 - \lambda_0\left(\frac{z_+ e N_{ref}}{J}\right)\right]. \qquad (9.6)$$

It is interesting to note the reappearance of the constants γ and M encountered elsewhere in our analysis.

In order to compare with the experimental data, we approximate $E_{bulk} = r\Delta V/L$, where ΔV is the applied potential difference, L the length of the cell, and $0 < r < 1$ accounts for potential drops in the double layers. Using the standard values for the $CuSO_4$ mobilities, $\mu_+ = 5.76 \times 10^{-4}$ cm^2/V sec and $\mu_- = 8.64 \times 10^{-4}$ cm^2/V sec [42], with $\Delta V = 6.0$ V, $L = 2.54$ cm, $\lambda_0 = 30$ μm, and $t_0 = 1$ sec, we estimate $t_c - t_i = 1.2$ sec for $r = 1$. For these conditions (see Fig. 3(c) of Ref. [29]), $t_c - t_i \approx 30$ sec, and t_i is on the order of seconds. If $r = 0.5$, then we estimate $t_c - t_i = 5.8$ sec. The discrepancy between our estimate and the observed value is probably due to the assumption of constant bulk field or the functional form of $N_-(x,t)$ being poor. The data does, however, seem loosely consistent with the dependence of $t_c - t_i$ on ΔV. A thorough test of our formulas should come from current data for a galvanostatic cell.

Rosso *et al.* provide a detailed theoretical and experimental description of the early moments of a galvanostatic $CuSO_4$ experiment, during the time $t < t_0$ when the depletion layer is forming [24]. Their data indicates a departure from the assumed concentration profile of Eq. (9.3) in that a slowly decaying tail is present due to gravity-induced convection, and the time t_0 is considerably larger than in the Cork *et al.* experiment. They do not, however, give concentration data for times $t > t_0$. If we use their data, $N_{ref} = 0.1$ M, $J = 40$ mA/cm^{-2}, $t_0 = 10$ sec, and $\lambda_0 = 0.1$ mm, then our formula predicts $t_c - t_i = 25$ sec, which might be consistent with the observed value of $t_c = 65$ sec.

Regardless of the accuracy of our estimates, the derivation is primarily intended to illustrate how the idea of a critical diffusion layer width as a prerequisite for ramified growth can be used to estimate the induction time. An analytical or numerical solution of the full transport equations could produce the correct result and would shed light on the validity of our assumptions. An interesting aspect of the derivation is the crucial role of the anions in regulating the formation of the diffusion layer. Barkey *et al.* present a surface instability calculation in which the diffusion layer width also directly influences the instability itself [15]. Thus, we see that the anions, whose role in controlling the speed of established growth is well understood, also play a role in regulating the onset of ramified growth.

X. CONCLUSION

We have solved for the concentration and potential profiles of the diffusion layer during ramified growth, and have derived from them ion fluxes and speeds. The solution is fairly general, allowing for different ion charges, mobilities and diffusion coefficients, nonzero concentration between the growth tips, and both potentiostatic and galvanostatic conditions. By considering the conservation of ions across the cell during wave propagation, we have determined the current compression factor, metal

ratio, and tip fraction. Finally, an estimate of the induction time for ramified growth has been given.

A complete analytic solution for ramified growth can be obtained by matching our solution for the diffusion layer to solutions for the active region near the growth and the region near the anode, where concentration builds up during deposition. Such a solution could predict electrical properties of the entire cell. Particular care must be taken in matching with the active region because it is the source of interesting effects like current oscillations during potentiostatic experiments [7,13], in addition to its primary role in morphology selection [17]. Fleury *et al.* present an analytic solution for the electric field and fluid velocity in the active region that describes the experimentally observed funnels, but we cannot easily match our solutions because they assume constant concentration ($N_{OCH} = N_{ref}$) and do not provide the constant in the electrostatic potential. The latter must be derived from a careful description of deposition kinetics. The Fleury solution could be modified to include effective boundary conditions on the concentration, potential and fluid velocity [34], which themselves express matching with the space charge layers, in order to determine exactly how space charge drives the vortices that comprise the funnels. The primary aim in matching various regions to obtain a complete solution for ramified growth in a binary electrolyte would be to directly link morphological characteristics of the growth (e.g., the filament spacing in dense-parallel growth) to fundamental properties of the electrolyte (e.g., $\kappa_{\pm}$, $\mu_{\pm}$, and $z_{\pm}$) as well as the current and applied potential.

ACKNOWLEDGMENTS

This work was funded in part by a Computational Science Graduate Program grant from the Office of Scientific Computing of the Department of Energy. The author thanks Bruce Bayly as well as Wing Tam and Jonah Erlebacher for helpful discussions and references.

[1] V. Fleury, M. Rosso, J.-N. Chazalviel, and B. Sapoval, Phys. Rev. A **44**, 6693 (1991).
[2] E. Ben-Jacob and P. Garik, Nature **343**, 523 (1990).
[3] R. M. Brady and R. C. Ball, Nature **309**, 225 (1984).
[4] V. Fleury, M. Rosso, and J.-N. Chazalviel, Phys. Rev. A **43**, 6908 (1991).
[5] D. Grier, E. Ben-Jacob, R. Clarke, and L. M. Sander, Phys. Rev. Lett. **56**, 1264 (1986).
[6] D. Grier, D. A. Kessler, and L. M. Sander, Phys. Rev. Lett. **59**, 2315 (1987). (1990).
[7] C. Livermore and P. Wong, Phys. Rev. Lett. **72**, 3847 (1994).
[8] M. Matsushita, M. Sano, Y. Hayakawa, H. Honjo, and Y. Sawada, Phys. Rev. Lett. **53**, 286 (1984).
[9] L. M. Sander, in *The Physics of Structure Formation*, edited by W. Guttinger and G. Dangelinayr (Springer, New York, 1984), pp. 257–266.
[10] J. R. Melrose, D. B. Hibbert, and R. C. Ball, Phys. Rev. Lett. **65**, 3009 (1990).
[11] Y. Sawada, A. Dougherty, and J. P. Gollub, Phys. Rev. Lett. **56**, 1260 (1986).
[12] P. P. Trigueros, F. Sagués, and J. Claret, Phys. Rev. E **49**, 4328 (1994).
[13] M. Wang and N. Ming, Phys. Rev. A **45**, 2493 (1992).
[14] R. Aogaki and T. Makino, J. Chem. Phys. **81**, 2154 (1984).
[15] D. P. Barkey, R. H. Muller, and C. W. Tobias, J. Electrochem. Soc. **136**, 2207 (1989).
[16] J. L. Barton and J. O'M. Bockris, Proc. R. Soc. London, Ser. A **268**, 485 (1962).
[17] J. Erlebacher, P. C. Searson, and K. Sieradzki, Phys. Rev. Lett. **71**, 3311 (1993).
[18] T. C. Halsey and M. Liebig, J. Chem. Phys. **92**, 3756; Phys. Rev. A **46**, 7793 (1992).
[19] T. A. Witten and L. M. Sander, Phys. Rev. Lett. **47**, 1400 (1981).
[20] W. Y. Tam and J. J. Chae, Phys. Rev. A **43**, 4528 (1991).
[21] J. S. Newman, *Electrochemical Systems* (Prentice-Hall, Englewood Cliffs, NJ, 1991).
[22] D. P. Barkey, P. Garik, E. Ben-Jacob, B. Miller, and B. Orr, J. Electrochem. Soc. **139**, 1044 (1992).
[23] J.-N. Chazalviel, Phys. Rev. A **42**, 7355 (1990).
[24] M. Rosso, J.-N. Chazalviel, V. Fleury, and E. Chassaing, Electrochim. Acta **39**, 507 (1994).
[25] J. S. Newman, J. Heat Mass Transfer **10**, 983 (1967).
[26] V. Fleury, J.-N. Chazalviel, and M. Rosso, Phys. Rev. Lett. **68**, 2492 (1992).
[27] J. S. Newman, Ind. Eng. Chem. Fundam. **5**, 525 (1966).
[28] D. Barkey, J. Electrochem. Soc. **138**, 2912 (1991).
[29] R. H. Cork, D. C. Pritchard, and W. Y. Tam, Phys. Rev. A **44**, 6940 (1991).
[30] D. B. Hibbert and J. R. Melrose, Proc. R. Soc. London Ser. A **423**, 149 (1989).
[31] D. P. Barkey and P. D. LaPorte, J. Electrochem. Soc. **137**, 1655 (1990).
[32] D. P. Barkey, D. Watt, Z. Liu, and S. Raber, J. Electrochem. Soc. **141**, 1206 (1994).
[33] V. Fleury, J.-N. Chazlviel, M. Rosso, and B. Sapoval, J. Electroanal. Chem. **290**, 249 (1990).
[34] B. J. Bayly, M. Z. Bazant, J. J. Chae, and W. Y. Tam (unpublished).
[35] P. Garik, D. Barkey, E. Ben-Jacob, E. Bochner, N. Broxholm, B. Miller, B. Orr, and R. Zamir, Phys. Rev. Lett. **62**, 2703 (1989).
[36] J. O'M. Bockris and A. K. N. Reddy, *Modern Electrochemistry* (Plenum, New York, 1970), Vol. 1, Chap. 4.
[37] C. M. Bender and S. A. Orszag, *Advanced Mathematical Methods for Scientists and Engineers* (McGraw-Hill, New York, 1978).
[38] M. W. Mullins and R. Sekerka, J. Appl. Phys. **34**, 323 (1963).
[39] V. Fleury, J. H. Kaufman, and D. B. Hibbert, Nature **367**, 435 (1994).
[40] N. Hecker, D. G. Grier, and L. M. Sander, in *Fractal*

Aspects of Materials, edited by R. B. Laibowitz, B. B. Mandelbrot, and D. E. Passoja (Materials Research Society, University Park, PA, 1985).

[41] A. J. Bard and L. R. Faulkner, *Electrochemical Methods* (John Wiley, New York, 1980).

[42] H. S. Harned and B. B. Owen, in *The Physical Chemistry of Electrolytic Solutions*, edited by W. A. Hamor (Reinhold, New York, 1958), p. 697.